Combined use of remote sensing and geostatistical data sets for estimating the dynamics of shortwave radiation of bare arable soils in Europe

Jerzy Cierniewski, Jakub Ceglarek, Cezary Kaźmierowski, Jean-Louis Roujean

▶ **To cite this version:**

Jerzy Cierniewski, Jakub Ceglarek, Cezary Kaźmierowski, Jean-Louis Roujean. Combined use of remote sensing and geostatistical data sets for estimating the dynamics of shortwave radiation of bare arable soils in Europe. International Journal of Remote Sensing, 2018, 40 (5-6), pp.2359-2374. 10.1080/01431161.2018.1474530 . hal-02354394

HAL Id: hal-02354394
https://hal.science/hal-02354394

Submitted on 16 Sep 2021

HAL is a multi-disciplinary open access archive for the deposit and dissemination of scientific research documents, whether they are published or not. The documents may come from teaching and research institutions in France or abroad, or from public or private research centers.

L'archive ouverte pluridisciplinaire **HAL**, est destinée au dépôt et à la diffusion de documents scientifiques de niveau recherche, publiés ou non, émanant des établissements d'enseignement et de recherche français ou étrangers, des laboratoires publics ou privés.

Distributed under a Creative Commons Attribution 4.0 International License

International Journal of Remote Sensing

ISSN: 0143-1161 (Print) 1366-5901 (Online) Journal homepage: https://www.tandfonline.com/loi/tres20

Combined use of remote sensing and geostatistical data sets for estimating the dynamics of shortwave radiation of bare arable soils in Europe

Jerzy Cierniewski, Jakub Ceglarek, Cezary Kaźmierowski & Jean-Louis Roujean

To cite this article: Jerzy Cierniewski, Jakub Ceglarek, Cezary Kaźmierowski & Jean-Louis Roujean (2019) Combined use of remote sensing and geostatistical data sets for estimating the dynamics of shortwave radiation of bare arable soils in Europe, International Journal of Remote Sensing, 40:5-6, 2359-2374, DOI: 10.1080/01431161.2018.1474530

To link to this article: https://doi.org/10.1080/01431161.2018.1474530

© 2018 The Author(s). Published by Informa UK Limited, trading as Taylor & Francis Group.

Published online: 11 May 2018.

Submit your article to this journal

Article views: 746

View related articles

View Crossmark data

Citing articles: 6 View citing articles

Full Terms & Conditions of access and use can be found at
https://www.tandfonline.com/action/journalInformation?journalCode=tres20

INTERNATIONAL JOURNAL OF REMOTE SENSING
2019, VOL. 40, NOS. 5–6, 2359–2374
https://doi.org/10.1080/01431161.2018.1474530

Taylor & Francis
Taylor & Francis Group

OPEN ACCESS Check for updates

Combined use of remote sensing and geostatistical data sets for estimating the dynamics of shortwave radiation of bare arable soils in Europe

Jerzy Cierniewski[a], Jakub Ceglarek[a], Cezary Kaźmierowski[a] and Jean-Louis Roujean[b]

[a]Department of Soil Science and Remote Sensing of Soils, Adam Mickiewicz University in Poznań, Poznań, Poland; [b]Centre National de Recherches Météorologiques, Météo-France/CNRS, Toulouse Cedex, France

ABSTRACT

Smoothing rough ploughed soils increases their albedo, which results in a lower amount of shortwave radiation being absorbed by their surface layer. That surface emits less longwave radiation, leading to a reduction in its temperature, which in turn can affect the climate. This article presents a multistage procedure using remote sensing and geostatistical data sets for quantification of the annual dynamics of shortwave radiation reflected from air-dried bare soils within arable lands of the European Union and its associated countries, Norway and Switzerland. The soils, being cultivated under conventional tillage, were treated as bare formed by a plough (Pd) and a smoothing harrow (Hs), when the major crops were planted there. Information about the areas of the soils and periods when they are bare was obtained from vectorized and rasterized geostatistical data sets. The spatial diversity of the spectral reflectance of the soils, characterized by thousands of their reflectance spectra (stored in the European Land Use and Cover Area frame Survey Top Soil Database), were used to predict the half-diurnal albedo variation of the soils on a given day of the year. The shortwave radiation reaching the examined soils was obtained from satellite data of the Spinning Enhanced Visible and Infrared Imager instrument. It was found that the maximum radiation levels reflected from the soils occur between the beginning of April and the end of May. During these periods, the radiation reflected from the soils formed by Pd and Hs can reach about 220 and 250 PJ d^{-1} in the western part of the EU, 150 and 190 PJ d^{-1} in the central part, and up to 280 and 330 PJ d^{-1} in the southern part.

ARTICLE HISTORY
Received 24 November 2017
Accepted 25 April 2018

1. Introduction

The overall level of the broadband albedo of bare soils depends on the content of soil pigments (soil organic carbon, iron oxides, and carbonates) (Ben-Dor, Irons, and Epema 1999) in their surface horizons. These soil properties are considered to be stable over time as opposed to soil moisture content and surface roughness, which change dynamically. Particularly intensive changes of bare soil roughness during the year are observed on arable soils that are in conventional tillage (Vaudour, Baghdadi, and Gilliot

CONTACT Jerzy Cierniewski ciernje@amu.edu.pl Department of Soil Science and Remote Sensing of Soils, Adam Mickiewicz University in Poznań, Poznań 61-680, Poland

© 2018 The Author(s). Published by Informa UK Limited, trading as Taylor & Francis Group.
This is an Open Access article distributed under the terms of the Creative Commons Attribution-NonCommercial-NoDerivatives License (http://creativecommons.org/licenses/by-nc-nd/4.0/), which permits non-commercial re-use, distribution, and reproduction in any medium, provided the original work is properly cited, and is not altered, transformed, or built upon in any way.

(2014). The albedo of dark-coloured, wet, and very rough soils ranges between 0.05 and 0.15, while the albedo of light-coloured, dry, and smooth soils varies between 0.35 and 0.40 (Dobos 2006; Oke 1992). Light-coloured crop residues can markedly raise the albedo level of dark-coloured soils (Horton et al. 1996). Soil surfaces with a deep groundwater table beneath quickly become dry after the rain, achieving the air-dry moisture state, which increases their reflectance. The spectral reflectance of soil surfaces with large irregular aggregates is lower than that of the same soil with more spherical and smaller aggregates (Mikhajlova and S. Orlov 1986). Matthias et al. (1991) reported that the spectral response of ploughed soils compared to their smoothed surfaces is about 25% lower. The kinetic energy of raindrops or water drops (produced by the sprinklers) also causes these soil surfaces to become smoother, increasing the reflectance of the soils by about 20–30% (Potter and Cruse 1987; Cierniewski 1999; Cierniewski 2001). The crust, formed as a result of the repeated wetting and drying of soil surfaces, reduces their roughness (Baumgardner et al. 1986; Bresson and Moran 2004; Cipra et al. 1971).

The albedo of soils, similarly to other land surfaces, varies during the day with the changing solar zenith angle (θ_s), reaching its minimum at the local noon (Monteith and Szeicz 1961; Lewis and Barnsley 1994; Wang et al. 2005; Oguntunde, Ajayi, and Van De Giesen 2006) and approaches 1.00 at the lowest position of the sun, when the sun rises and sets. Cierniewski et al. (2015) found that soil roughness affected not only the overall level of those variations, but also the intensity of its increase from θ_s at the local noon to about 75–80°. Surfaces of rough and deeply ploughed soils showed almost no rise in albedo values at θ_s lower than 75°, while the same soil, but smoothed, exhibited a gradual albedo increase at these angles. Cierniewski et al. (2017) proposed equations for calculating the diurnal variation of the broadband blue-sky albedo of soils with respect to their roughness based on their spectra obtained in laboratory conditions. Those spectra are stored in the Global Soil Spectral Library and the Land Use and Cover Area frame Survey (LUCAS) – European Soil Portal (Tóth, Jones, and Montanarella 2013; Viscarra Rossel et al. 2009). Viscarra Rossel et al. (2016) indicated that the information coded in the spectra collected there could be used to investigate the spatial variation of standard soil properties, but also that those soil spectra can be used to assess and monitor soils as surfaces affecting the climate of the Earth on a regional and global scale, provided the perturbing factors of soil surface condition be neglected.

Studies on the albedo variation of soils, like that of other land surfaces, seem to be particularly relevant in the context of statements made by Sellers et al. (1995), which say that global climate models require an albedo accuracy higher than ±2%. The albedo of soils, affecting the energy transfer between soil, vegetation, and the atmosphere, is also used as input data in the modelling of global climate (Ben-Gai et al. 1998; Schneider and Dickinson 1974). The use of different agricultural tools changes the amount of shortwave radiation absorbed by cultivated soils, leading to a change in their temperature and emission of longwave radiation, which in turn can affect the climate (Davin, de Noblet-Ducoudré, and Friedlingstein 2007; Desjardins 2007, Farmer and Cook 2013).

In order to accurately model the processes associated with the flow of radiation between the Earth's surface and the atmosphere for periods longer than a few days, the average daily value of the albedo seems to be more useful than instantaneous values. To obtain this average value, the knowledge of a daily albedo variation is needed (Grant, Prata, and Cechet 2000; Cierniewski et al. 2013; Cierniewski et al. 2015). Cierniewski, Królewicz, and Kaźmierowski

(2017) have used the average diurnal albedo values of soils within arable lands in Poland to quantify the annual dynamics of shortwave radiation reflected from them as a consequence of the smoothing of previously ploughed and harrowed soils.

This article presents a multistage procedure, employing remote-sensing data (laboratory reflectance spectra of bare soils and the solar reflective radiation reaching the studied area obtained by satellite technology) as well as geostatistical data sets (describing the spatial distribution and acreage of the major crops), which aim to quantify the annual dynamics of the shortwave radiation reflected from bare soils within the arable lands of the European Agricultural Region (EAR). This dynamic refers to soils that undergo conventional tilling when they are prepared for planting major crops, when they are not covered by the crops and their residues in degree, which can significantly change the bare soil's reflectance features. To assess the impact of the roughness of the analysed soils on this dynamic, it was assumed that they are in two extreme roughness states formed by a plough and a smoothing harrow. In addition, to simplify this procedure, it was assumed that the soils are air-dried.

2. Study area and methods

The procedure presented in this article is shown in the flow chart (Figure 1), with all the steps explained in this section. The study area is the EAR according to the Major World Crop Areas and Climate Profiles (USDA 1994). It is limited to the current member countries of the European Union (EU), together with its associated countries (Switzerland and

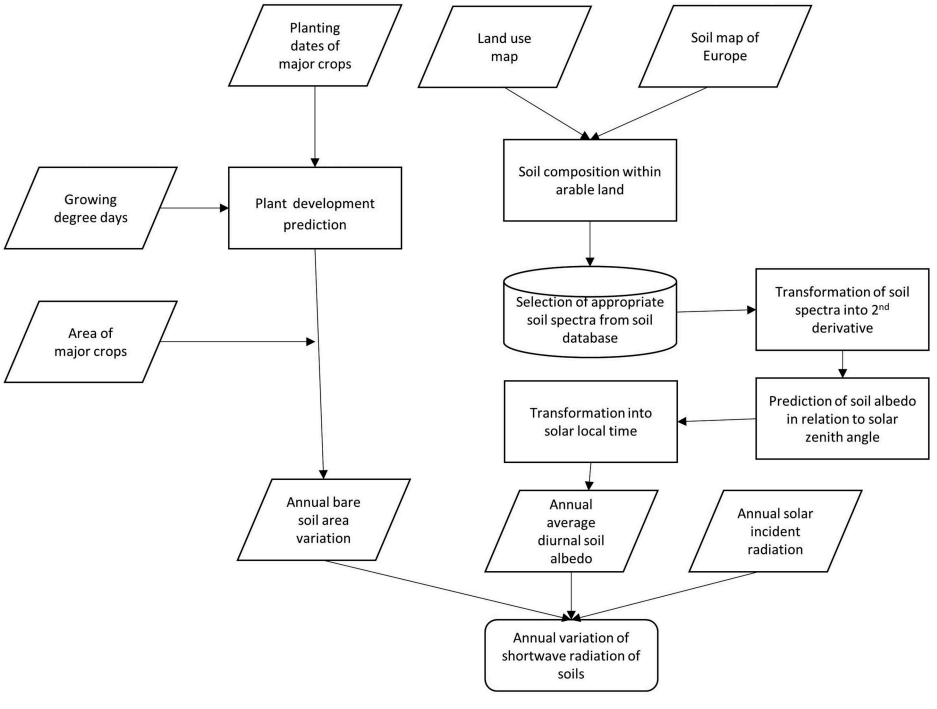

Figure 1. General flow chart used in the procedure.

Norway). Due to the variability of climatic conditions in such a wide area, resulting from diversity of crop development conditions, and the inclusion of statistics on the share of arable land areas in conventional tillage in individual EU countries, the EAR was analysed after being divided into western (W), central (C), and southern (S) subregions (Figure 2).

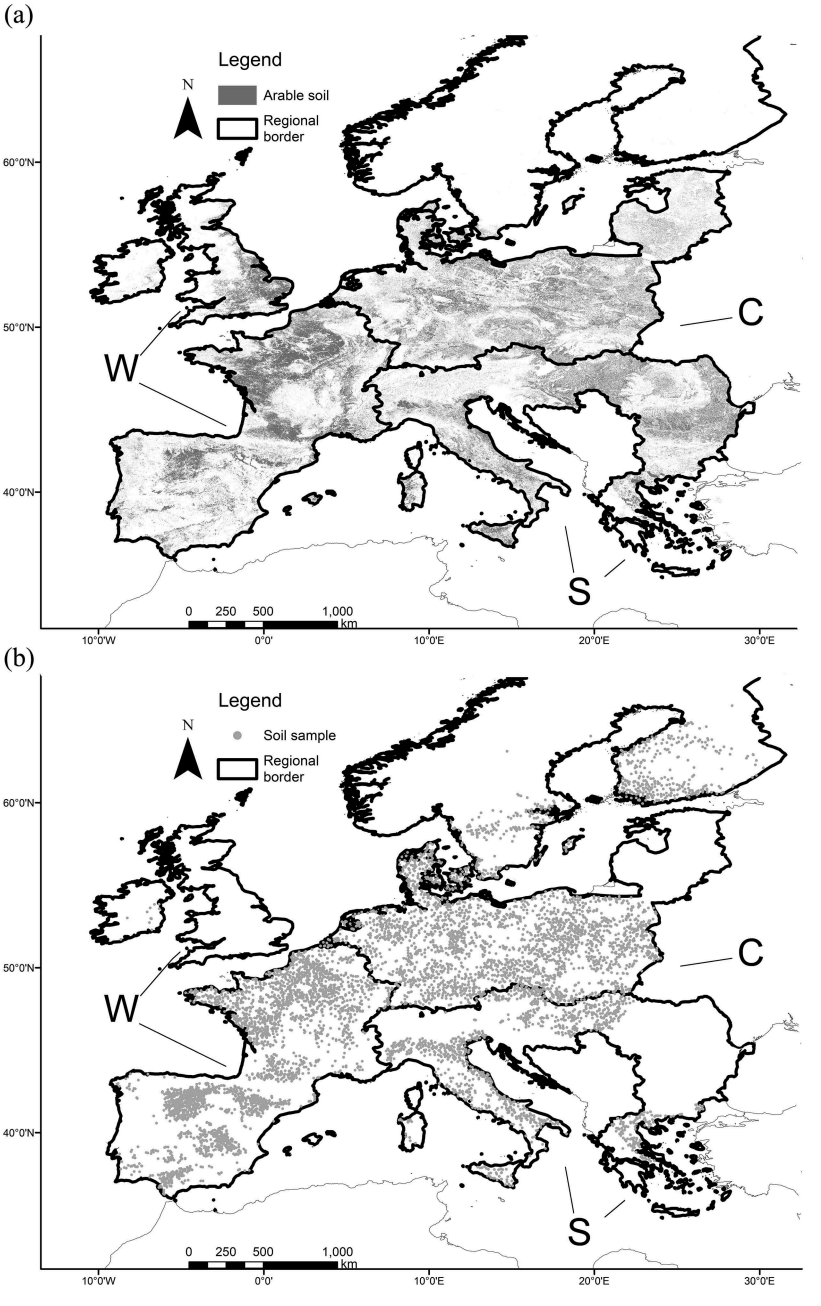

Figure 2. Subregions where the major crops occur and soils can be bare (a) and showing the location of the soil samples from which the laboratory reflectance spectra were used to predict the albedo of the soils (b).

In the first stage of the procedure, the spatial distribution and acreage of the major crops cultivated in each subregion were assessed. The data set of the geographic distribution of crops (Monfreda, Ramankutty, and Foley 2008) was used to determine dominant crops in each of the three subregions. The data set, in the form of a raster image with a pixel size of 5 × 5 arcmin (roughly 10 × 10 km, latitude dependent), contains the area in hectares used for the cultivation of major crops within the aforementioned pixel. Besides calculating the area and the share of the major crops within the subregions, the data set also helped to pinpoint the central agricultural location of each subregion.

The Crop Calendar Dataset (Sacks et al. 2010), which contains digitalized and georeferenced observations of crop planting and harvesting days (also with the resolution of 5 × 5 arcmin), was also used in this first stage. The data set, together with the previous one, both spanning the whole globe, were delimited to the three analysed subregions. Inside each of them, the geographic distribution and the crop calendar were intersected, outputting the planting days for each crop together with its acreage.

Having the planting days and the acreage pinpointed, the periods when soil would stay bare after planting were calculated. Growing degree days (GDDs) were used in order to find the duration in which any given crop would take to grow and overtake the spectral characteristics of bare soil. This was adopted in accordance with the suggestion of Baumgardner et al. (1986), who stated that soil starts to exhibit vegetal spectral characteristics when vegetation covers more than 15% of its surface. For each of the subregions, average daily temperatures, based on mean results from 10 years, were obtained from the National Center for Atmospheric Research (NCAR (National Center for Atmospheric Research) 2017). Centre points, related to the geographic distribution of farmlands in each subregion, found in the first stage, were used to extract the aforementioned temperatures. GDDs were calculated individually for various crops, depending on the base temperature. Therefore, various annual cumulative GDD distributions were calculated to assess the development of selected crops. Having the planting dates of the crops, together with the GDD distributions, it was possible to estimate time windows throughout the year when the crops have not yet covered 15% of the soil surface. The proper amount of the cumulated GDD required to reach the aforementioned threshold percentage for each of the major crops was found, following the recommendations of Miller, Lanier, and Brandt (2001), Worthington and Hutchinson (2005), and Lee (2011). Using ArcMap developed by the Environmental Systems Research Institute, the maps of the crop planting dates and the crop harvesting areas were overlaid, and the acreage of the previously found bare soils was obtained.

In the second stage of the procedure, to determine the soil units that the delineated arable areas belong to, a digital soil map (ESDB v2.0 2004), classified as major reference groups according to the World Reference Base (WRB) for Soil Resources, was superimposed on the croplands class taken from a land-cover map (GlobCover 2009). The croplands class from the land-cover map was selected to highlight soils used for farming and extract their area in all of the subregions. In the third stage, the soil units that occupied more than 5% of the area of the arable soils in a given subregion were characterized by the reflectance spectra of all the soil samples that were located in their contours. The spectra were obtained from the European LUCAS Top Soil Database (Tóth, Jones, and Montanarella 2013). Laboratory reflectance spectra related to 2482, 2373, and 968 soil samples taken from W, C, and S, respectively, were used to characterize the reflectance features of the major groups of soils within these subregions.

These average spectra of the analysed subregions were used in the fourth stage to calculate the half-diurnal albedo (α) variation of the bare soils within W, C, and S. Their overall soil α level at a given roughness condition under the $\theta_s = 45°$ (α_{45}) was calculated as in the paper proposed by Cierniewski, Ceglarek, and Kaźmierowski (Forthcoming):

$$\alpha_{45} = 0.33 - 0.1099\,T_{3D} - 5,795.4\,d_{574} - 510.2\,d_{1087} + 7,787.2\,d_{1355} + 1,2161\,d_{1656} + 6,32.8\,d_{698}, \quad (1)$$

where T_{3D} is the roughness index defined as the ratio of the real surface area within its basic unit to its flat horizontal area (Taconet and Ciarletti 2007), and d stands for the reflectance data transformed to its second derivative and wavelengths selected for a specified wavelength: 574, 698, 1087, 1355, and 1656 nm by Savitzky–Golay filter using software stepwise procedure in the Statistical Package for the Social Sciences. These wavelengths were selected from the range between 400 and 2500 nm, based on 153 samples from France, Poland, and Israel. Meanwhile, α_{θ_s} under θ_s <75° was calculated as

$$\alpha_{\theta_s} = \alpha_{45}[1 + s_\alpha(\theta_s - 45)], \quad (2)$$

where s_α expresses the slope of the α increases in this θ_s range:

$$s_\alpha = 0.000000626 + 0.0043(\mathrm{HSD})^{-1.418}, \quad (3)$$

where HSD is the roughness index expressing the standard deviation of the height of a soil surface area within its basic unit (Taconet and Ciarletti 2007). The half-diurnal α variation of the soil units relative to θ_s, taking into account their roughness, was expressed in the full θ_s range up to 90° by the formula:

$$\alpha_{\theta_s} = \exp\left(\frac{a + c\,\theta_s}{1 + b\,\theta_s + d(\theta_s)^2}\right), \quad (4)$$

where *a, b,* and *c* are fitting parameters. This equation was individually fitted to the average half-diurnal α distributions of the bare soils, using TableCurve 2Dv5.01 software, assuming that each of them was shaped by a plough (Pd) and smoothing harrow (Hs) within W, C, and S. It was assumed that the roughness of the soils formed by Pd and Hs was described by HSD values of 25 and 5 mm, and T_{3D} values of 1.50 and 1.05, respectively.

In the fifth stage, these α_{θ_s} distributions of the soils representing W, C, and S in the full θ_s range were transformed to the function of solar local time (SLT) for every tenth day of the year (DOY). For simplicity, these transformations were made for centres of the subregions with the following coordinates: 46°12′N, 02°42′E for W, 51°42′N, 15°18′E for C, and 44°06′N, 23°18′E for S. These α distributions in the SLT function allowed us to predict the half-diurnal albedo variation of the soils in the analysed days and calculate their daily average values (α_d) for the days.

In the sixth stage, using three channels of the satellite Spinning Enhanced Visible and Infrared Imager instrument (related to 0.6, 0.8, and 1.6 μm), the amounts of shortwave radiation ($R_{i,d}$) reaching the centres of the subregions (located as described as above), characterizing W, C, and S for every day in 2011 (in increments of 1 h) in a clear sky and with varying degrees of cloudiness conditions, were determined. These amounts were obtained by a modified method implemented in the Satellite Application Facility on Land Surface Analysis project proposed by Gautier, Diak, and Masse (1980) and Frouin et al. (1989). To smooth the impact of highly variable atmospheric conditions, the daily $R_{i,d}$ values for W, C,

and S were averaged over the year by a non-linear Complementary Error Function Peak Equation implemented in TableCurve 2D v5 software as no. 8008 (Systat Software Inc., USA). Finally, $R_{i,d}$ values were converted to TJ km^{-2}. Multiplying the bare soil areas within W, C, and S by the α_d of the soils formed by Pd and Hs, as well as the $R_{i,d}$ values, the diurnal amount of shortwave radiation reflected from the subregions throughout the year was estimated ($R_{r,d}$).

3. Results

Barley, wheat, maize, potato, rye, sugar beet, and rapeseed are the major crops in the EAR. It was found that the total soil areas used for their cultivation in W, C, and S were about 229, 231, and 197 thousand square kilometres, respectively (Figure 2). Wheat, together with barley, has the largest share in the area of W, C, and S, exceeding 70%, 60%, and 50%, respectively (Table 1). Adding shares of maize and rapeseed in W and only maize in S to the participation of these two dominant cereals, these crops together cover over 90% in both of these two subregions. Maize has the smallest share of only 3% within C, and the share of such crops as rye, rapeseed, and potato is 14%, 9%, and 8% there, respectively. Taking into account the Eurostat data from 2013 (Eurostat. 2013), which state that the above areas are under conventional tillage in the proportions of 56%, 69%, and 74%, it was determined that the research areas within W, C, and S are 128, 160 and 146 thousand square kilometres, respectively.

The share of the WRB major soil groups, together covering at least 90% of each subregion, is shown in Table 2. *Cambisols* and *Luvisols* together have a dominant share of 66% and 56% in W and C, respectively. Although the proportion of *Cambisols* in S is larger than in W and C, the proportion of *Luvisols* is in the third position behind *Chernozems*. *Fluvisols* participation is also relatively high, reaching about 10% in each subregion. *Leptosols* in W, *Podsols* in C, and *Phaeozems* in S have similar shares between 8% and 11%. The shares of other soil units in each subregion do not exceed 5%.

The greatest diversity of soil spectral reflectance is between the averaged major soil groups in S, where their lowest reflectance refers to dark-coloured *Phaeozems* with a high content of soil organic matter (SOC), and the highest to light-coloured *Leptosols* with a much lower SOC content (Figure 3). Meanwhile, the smallest difference in the reflectance is revealed between the main groups in W, where the spectra of these six soil units refer to soils with similar contents of SOC and $CaCO_3$. Averaging the spectra of all soil units, weighting in the area occupied by them in a given subregion, resulted in these three averaged spectra (characterizing all soils within W, C, and S) being very similar to each other (Figure 4). Their similarity is also evident in their half-diurnal α distributions (in the full θ_s range from 0° to 90°), generated using Equations (1)–(4) as the surfaces formed by a Pd and a Hs (Figure 5).

Table 1. Proportion of the area covered by the major crops within W, C, and S subregions.

Crop	W (%)	C (%)	S (%)
Wheat	42.0	34.7	44.4
Barley	30.8	25.5	10.0
Maize	11.9	3.4	37.3
Potato	2.8	8.1	3.5
Rye	0.9	13.7	0.8
Sugar beat	3.9	5.1	2.7
Rapeseed	7.7	9.4	1.2

Table 2. Proportion of the area of the major WRB soil groups within W, C, and S subregions.

	W		C		S	
Soil unit	Area (%)	Number of contours	Area (%)	Number of contours	Area (%)	Number of contours
Albeluvisol	4.1	303	4.2	345	N/A	N/A
Arenosol	N/A	N/A	4.7	407	N/A	N/A
Cambisol	43.0	2503	22.4	1386	28.8	1360
Chernozem	N/A	N/A	N/A	N/A	19.2	254
Fluvisol	8.9	596	9.3	612	10.7	304
Gleysol	N/A	N/A	4.2	389	N/A	N/A
Leptosol	8.2	627	N/A	N/A	3.3	633
Luvisol	22.8	1105	34.0	1,429	14.7	715
Phaeozems	N/A	N/A	3.1	121	11.1	267
Podzol	N/A	N/A	9.9	903	N/A	N/A
Regosol	2.9	247	N/A	N/A	N/A	N/A
Vertisol	N/A	N/A	N/A	N/A	3.1	107

N/A: not applicable.

The overall level of the half-diurnal α distributions of the averaged soils within the subregions, related to the soil surfaces formed by a Hs, is clearly higher than the surfaces shaped by a Pd. Figure 6 shows examples of digital elevation models (DEMs) of the soil surfaces studied in Poland formed by a plough and a smoothing harrow, which were described by the roughness indices, HSD and $T_{3D,}$ with similar values to those used in Equations (1)–(3). The α values all of the averaged smooth soil surfaces increase by about 18% when the θ_s grows from 30° to 75°. The α at the θ_s of 45° for these smooth surfaces is higher by about 14% than those of very rough ones. Examples of the half-diurnal α distributions of the averaged soils within W, C, and S generated in the SLT function from noon to sunset for the shortest and longest days (at the beginning of the astronomical winter in the 173rd DOY and the astronomical summer in the 356th DOY), respectively, as well as for the day of its medium length (at the beginning of the astronomical spring or autumn in the 81st DOY or the 267th DOY), show how values of the average diurnal albedo (α_d) of soils vary with the soil surface roughness and the date (Figure 7). All of the distributions contain a longer section of low α values and a shorter section of a rapid α growth before sunset. The length of this shorter section is the same in all cases, referring to the same time interval. The length of the longer section depends on the date, but also on the latitude of a given surface. The section is evidently longer if the day is longer. For soil areas located at a higher latitude, the length of this section additionally increases from the 81st DOY to the 267th DOY, and decreases from the 267th DOY to the 81st DOY the following year. Thus, this longer section is significantly longer for the soils located in the highest latitude within C at the 173rd DOY than the 356th DOY. The level of this longer section rises with the local time for smooth surfaces (describing its increasing α values) as opposed to rough surfaces, whose level is almost unchanged over time. Since the α_d value of any soil surface depends on the proportion between the lengths of the shorter and the longer section, the longer the day, the longer the section with low α values, and the lower the α_d value,

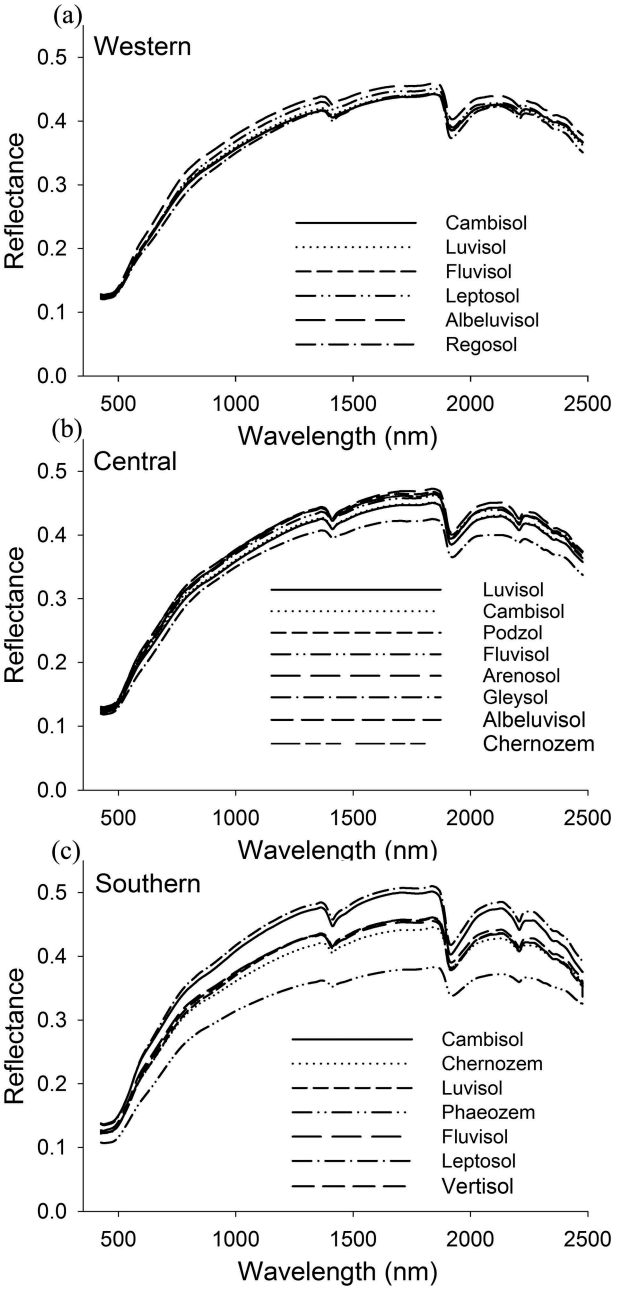

Figure 3. Averaged spectra of the major WRB soil groups within the analysed subregions.

which is particularly noticeable for smooth surfaces. The α_d values of the surfaces shaped by a Hs, shown in Figure 7, are higher by about 14%, 16%, and 18% than that of rough surfaces formed by a Pd, in the 173rd DOY, the 267th (or the 81st DOY), and the 356th, respectively, regardless of the location of their surface (Table 3).

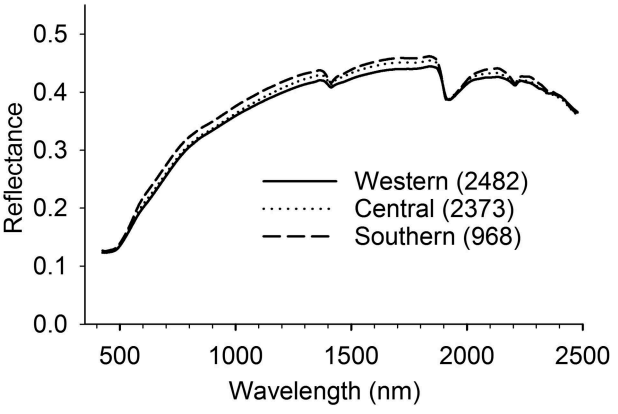

Figure 4. Spectra of averaged soils within the analysed subregions with analysed soil samples (in parenthesis).

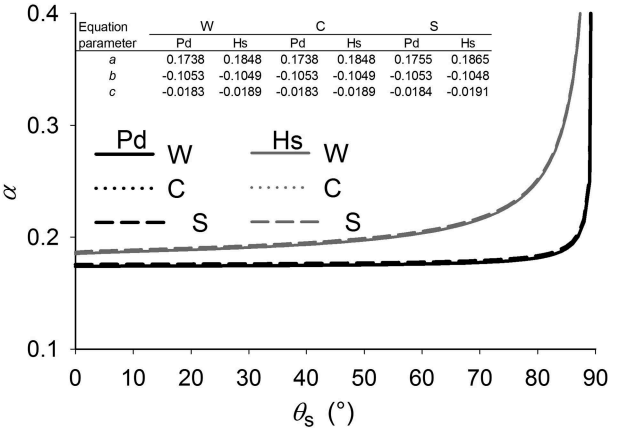

Figure 5. Distribution of a over the whole θ_s from 0° to 90° for averaged bare soils within the W, C, and S subregions, generated as formed by a Pd, and a Hs by Equation (4) with the fitting parameters *a, b*, and *c*.

This annual variation of α_d values of the averaged soils within the studied subregions can be seen in Figures 8(a)–(c).

The annual distributions of the bare soil areas within the analysed subregions (Figures 8(d)–(f)) are the result of the aggregation of the bare soil areas related to the individual major crops present in these subregions. Spring peaks of the bare soil areas, about 85,000 and 60,000 km^2, were found within W and C around the 95th DOY (5 April) and the 125th DOY (5 May), respectively. The largest spring peak, reaching 95,000 km^2, was established within S around the 110th DOY (20 April). Significantly smaller autumn peaks of the bare soil areas within W, C, and S, reaching 10,000, 20,000, and less than 5000 km^2, respectively, were found around the 280th DOY (7 October). Within S in summer around the 210th DOY an additional area of bare soils was found measuring 10,000 km^2. The diurnal amount of the $R_{i,d}$, reaching the subregions in 2011 varied from about 2 TJ km^{-2} around the beginning of the astronomical winter to 17,

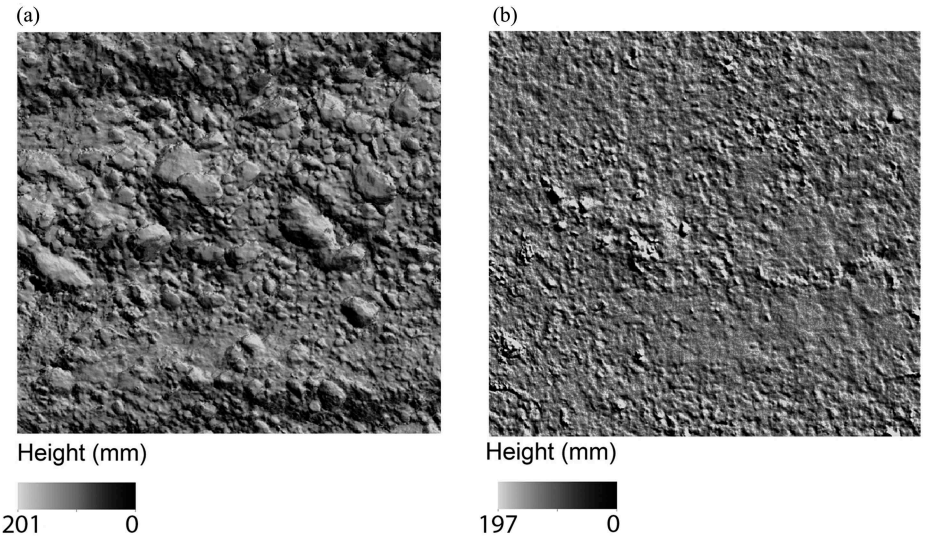

Figure 6. DEM of the soil surface: (a) formed by a Pd with the values of HSD = 25.65 mm and roughness T_{3D} = 1.54; (b) formed by a Hs with the values of HSD = 2.97 mm and roughness T_{3D} = 1.06, located in Poland (52°35′50″N, 16°38′05″E) and classified as *Luvisol*.

19, and 21 TJ km^{-2} for C, W, and S, respectively, at the beginning of the astronomical summer (Figures 8(g)–(i)). The spring maxima of the $R_{r,d}$ that can be reflected from the bare soils in W, C, and S were predicted from the beginning of April to the end of May at 90–125th DOY, 120–140th DOY, and 110–150th DOY, respectively (Figures 8(j)–(l)). During these periods, $R_{r,d}$ related to the soils formed by Pd and Hs can reach about 220 and 250 PJ day^{-1} in W, 150 and 190 PJ day^{-1} in C, and up to 280 and 330 PJ day^{-1} in S. At the turn of summer and autumn, between 240th DOY and 280th DOY (from the end of August to the beginning of October), the radiation amount reflected from bare soils formed by Pd and Hs can reach only 20–25 PJ day^{-1} in W and 25–30 PJ day^{-1} in C. The radiation in this period in S can be almost imperceptible. In contrast, in summer around the end of July, the radiation in S can reach 25 and 30 PJ day^{-1} for Pd and Hs, respectively.

4. Discussion

In the presented procedure, aimed at estimating the dynamics of the $R_{r,d}$ of bare soils within the arable lands of the EU, the statistical data on the share of arable land in conventional tillage (S_A) was also used along with geostatistical data sets. These S_A were obtainable from Eurostat in relation to individual EU countries, showing large differences between them (Eurostat. 2017). For example, in 2013, S_A values determining the areas of bare soils in large areas of arable land within the delineated subregions were obtained as follows: Spain (71%) and France (49%) within W, Poland (86%) and Germany (57%) within C, and Romania (82%) and Italy (74%) within S. These S_A values allow the realistic limiting of the areas of arable lands which were established on the basis of the geostatistical data sets in the first stage of the procedure to those that were ploughed

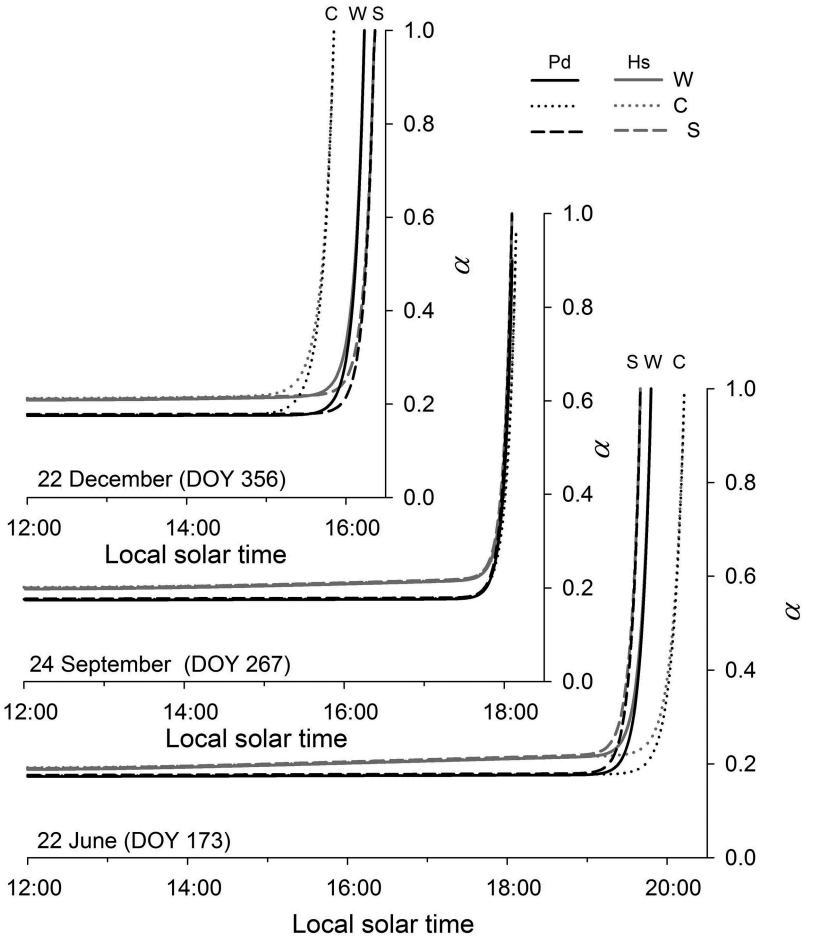

Figure 7. Half-diurnal *α* distribution of the average bare soils within the subregions formed by a Pd, and a Hs, generated in relation to the solar local time in three selected days of the year.

Table 3. Average diurnal albedo value (α_d) of the averaged soils formed by Pd and Hs within W, C, and S subregions in the following DOY: 173rd, 267th, and 356th.

		W: 46°12′N		C: 51°42′N		S: 44°06′N	
Day length (h)	DOY	Pd	Hs	Pd	Hs	Pd	Hs
>14	173	0.186	0.212	0.189	0.216	0.188	0.214
12	267	0.187	0.217	0.191	0.222	0.190	0.222
>7	356	0.197	0.233	0.206	0.243	0.200	0.235

before planting major crops under conventional tillage and can therefore be treated as bare soils within short time periods. Because the $R_{r,d}$ of the soils was calculated using the albedo of soil samples collected from arable land within each of the European agricultural subregions, and their albedo was predicted through their reflectance spectra stored in soil databases, it was also assumed that arable land during these short periods is not covered with crops or any of their residues. With the intention of taking into

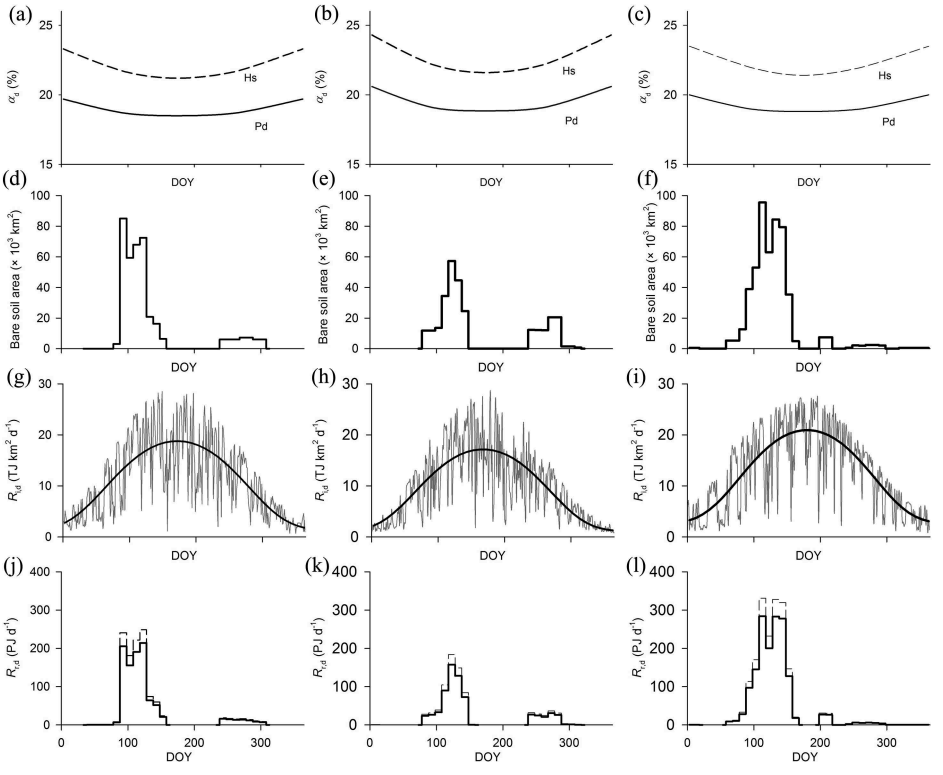

Figure 8. Annual variations within the W, C, and S subregions (from left column to right one) in (a–c) average diurnal albedo (a_d) of the averaged bare soils formed by a Pd and a; (d–f) areas of the bare soils; (g–i) real (grey line) and averaged (black line) $R_{i,d}$ reaching the soils; (j–l) $R_{r,d}$, formed by a Pd (solid black line) and a Hs (dotted grey line).

account the variability of S_A values obtained with such a low spatial resolution, especially for the largest EU countries mentioned above, the boundaries between the three European agricultural subregions were also determined based on the course of the borders of EU countries and, of course, climate differentiation.

The annual variation of the bare soil area within C, with two peaks, is similar to that established for Poland alone using Landsat 8 data (Cierniewski, Królewicz, and Kaźmierowski 2017). While the spring peak within W is significantly higher than its autumn peak, both peaks in Poland are of a similar magnitude. The clearly dominant peak representing the maximum area of bare soils within S in Europe shows similarities to the corresponding peaks established for the arable land in Israel, although the former occurs in spring and the latter at the turn of summer and autumn (Cierniewski et al. Forthcoming).

Using the procedure proposed here, based on the soil reflectance spectra that are commonly collected around the world and stored in soil databases, the authors of this article also intend to estimate the amount of shortwave radiation that could be reflected from bare soils within arable lands throughout the year on a global scale. In this way, the authors would like to expand the field of application of the aforementioned data sets to the analysis of the impact of soils on the Earth's

climate on a regional and global scale, as mentioned by Viscarra Rossel et al. (2016).

5. Concluding remarks

The results presented in this article show a clear annual variation of the amount of shortwave radiation reflected from bare soils within arable lands in the EU.

It was found that the greatest amount of radiation could be reflected from the soils from the beginning of April to the end of May. This instantaneous radiation amount of the soil shaped by a smoothing harrow and a plough was estimated at 250 and 220 PJ day^{-1}, respectively, for the western part of the EU, 190 and 150 PJ day^{-1} for the central part, and 330 and 280 PJ day^{-1} for the southern part. This study indicates that the quantitative relationship between the reflectance of soils and their blue-sky albedo variation requires further research on arable lands in larger areas to evaluate the impact of bare soil reflection on a global scale.

The procedure proposed in this article confirms the suggestion of Viscarra Rossel et al. that the data stored in soil databases could also be used to study the effect of soils on the Earth's climate.

Acknowledgments

This work was supported by the Polish National Science Centre as part of the framework of project no. 2014/13/B/ST10/02111.

Disclosure statement

No potential conflict of interest was reported by the authors.

Funding

This work was supported by the Polish National Science Centre as part of the framework of [Project No. 2014/13/B/ST10/02111].

References

Baumgardner, M. F., L. F. Silva, L. L. Biehl, and E. R. Stoner. 1986. "Reflectance Properties of Soils." *Advances in Agronomy* 38: 1–44. doi:10.1016/S0065-2113(08)60672-0.

Ben-Dor, E., J. R. Irons, and G. F. Epema. 1999. "Soil Reflectance." In *Remote Sensing for the Earth Sciences, Manual of Remote Sensing*, edited by A. N. Rencz, 111–188. New York: Wiley & Sons.

Ben-Gai, T., A. Bitan, A. Manes, P. Alpert, and S. Rubin. 1998. "Spatial and Temporal Changes in Rainfall Frequency Distribution Patterns in Israel". *Theoretical and Applied Climatology* 61 (3–4). Springer-Verlag: 177–190. doi:10.1007/s007040050062.

Bresson, L. M., and C. J. Moran. 2004. "Micromorphological Study of Slumping in a Hardsetting Seedbed under Various Wetting Conditions." *Geoderma* 118 (3–4): 277–288. doi:10.1016/S0016-7061(03)00212-X.

Cierniewski, J. 1999. *Geometrical Modeling of Soil Bi-Directional Reflectance in the Optical Domain*. Poznan: Bogucki Scientific Publishers.

Cierniewski, J. 2001. *The Bidirectional Reflectance Model from Cultivated Soils Taking into Account Soil Aggregates and Micro-Relief (In Polish)*. Poznan: Bogucki Scientific Publishers.

Cierniewski, J., A. Karnieli, C. Kazmierowski, S. Krolewicz, J. Piekarczyk, K. Lewinska, A. Goldberg, R. Wesolowski, and M. Orzechowski. 2015. "Effects of Soil Surface Irregularities on the Diurnal Variation of Soil Broadband Blue-Sky Albedo." *IEEE Journal of Selected Topics in Applied Earth Observations and Remote Sensing* 8 (2): 493–502. doi:10.1109/JSTARS.2014.2330691.

Cierniewski, J., C. Kaźmierowski, S. Krolewicz, and J. Piekarczyk. 2013. "Effects of Soil Roughness on the Optimal Time of Cultivated Soils Observation by Satellites for the Soils Average Diurnal Albedo Approximation." *IEEE Journal of Selected Topics in Applied Earth Observations and Remote Sensing* 6 (3): 1194–1198. doi:10.1109/JSTARS.2012.2234440.

Cierniewski, J., J. Ceglarek, A. Karnieli, E. Ben-Dor, S. Królewicz, and C. Kaźmierowski. Forthcoming. "Shortwave Radiation Affected By Agricultural Practices." *Remote Sensing*.

Cierniewski, J., J. Ceglarek, A. Karnieli, S. Królewicz, C. Kaźmierowski, and B. Zagajewski. 2017. "Predicting the Diurnal Blue-Sky Albedo of Soils Using Their Laboratory Reflectance Spectra and Roughness Indices." *Journal of Quantitative Spectroscopy and Radiative Transfer* 200 (June): 25–31. doi:10.1016/j.jqsrt.2017.05.033.

Cierniewski, J., J. Ceglarek, and C. Kaźmierowski. Forthcoming. "Predicting the Diurnal Blue-Sky Albedo Variation of Soil with Given Roughness Using Their Hyperspectral Reflectance Spectra Obtained under Laboratory Conditions." *Remote Sensing*.

Cierniewski, J., S. Królewicz, and C. Kaźmierowski. 2017. "Annual Dynamics of Shortwave Radiation as Consequence of Smoothing of Previously Plowed and Harrowed Soils in Poland." *Journal of Applied Meteorology and Climatology* 36 (March): 735–743. doi:10.1175/JAMC-D-16-0126.1.

Cipra, J. E., M. F. Baumgardner, E. R. Stoner, and R. B. MacDonald. 1971. "Measuring Radiance Characteristics of Soil with a Field Spectroradiometer1." *Soil Science Society of America Journal* 35 (6): 1014. doi:10.2136/sssaj1971.03615995003500060043x.

Davin, E. L., N. de Noblet-Ducoudré, and P. Friedlingstein. 2007. "Impact of Land Cover Change on Surface Climate: Relevance of the Radiative Forcing Concept." *Geophysical Research Letters* 34 (13): n/a-n/a. doi:10.1029/2007GL029678.

Desjardins, R. L. 2007. "The Impact of Agriculture on Climate Change." *Adapting Agriculture to Climate Change*: 29–39. Accessed May 12, 2017. http://nabc.cals.cornell.edu/Publications/Reports/nabc_21/21_2_2_Dejardins.pdf

Dobos, E. 2006. "Albedo." In *Encyclopedia of Soil Science*, edited by R. Lal, 64–66. New York: Taylor & Francis.

European Commission. 2004. European Soil Database (v2.0 2004). Accessed September 5, 2017 https://esdac.jrc.ec.europa.eu

Eurostat. 2013. "General and Regional Statistics" Eurostat. Accessed October 10 2017. http://ec.europa.eu/eurostat

Farmer, T. G., and J. Cook. 2013. *Climate Change Sicence: A Modern Synthesis. Volume 1 – The Physical Climate*. Dordrecht: Springer. doi:10.1007/s13398-014-0173-7.2.

Frouin, R., D. W. Lingner, C. Gautier, K. S. Baker, and R. C. Smith. 1989. "A Simple Analytical Formula to Compute Clear Sky Total and Photosynthetically Available Solar Irradiance at the Ocean Surface." *Journal of Geophysical Research* 94 (C7): 9731. doi:10.1029/JC094iC07p09731.

Gautier, C., G. Diak, and S. Masse. 1980. "A Simple Physical Model to Estimate Incident Solar Radiation at the Surface from GOES Satellite Data." *Journal of Applied Meteorology*. doi:10.1175/1520-0450(1980)019<1005:ASPMTE>2.0.CO;2.

GlobCover. 2009. *Global Land Cover Map*. Paris: European Space Agency.

Grant, I. F., A. J. Prata, and R. P. Cechet. 2000. "The Impact of the Diurnal Variation of Albedo on the Remote Sensing of the Daily Mean Albedo of Grassland." *Journal of Applied Meteorology* 39 (2): 231–244. doi:10.1175/1520-0450(2000)039<0231:TIOTDV>2.0.CO;2.

Horton, R., K. L. Bristow, G. J. Kluitenberg, and T. J. Sauer. 1996. "Crop Residue Effects on Surface Radiation and Energy balance—Review." *Theoretical Applied Climatology* 54: 27–37. doi:10.1007/BF00863556.

Lee, C. 2011. "Corn Growth Stages and Growing Degree Days: A Quick Reference Guide." In *Cooperative Extension Service*, 2. Lexington: University of Kentucky, College of Agriculture.

Lewis, P., and M. J. Barnsley. 1994. "Influence of the Sky Radiance Distribution on Various Formulations of the Earth Surface Albedo." In Proc. 6th Int. Symp. Phys. Meas. Signatures Remote Sens, 707–716. Val d'Is.re.

Matthias, A. D. D., A. Fimbres, E. E. E. Sano, D. F. F. Post, L. Accioly, A. K. K. Batchily, and L. G. G. Ferreira. 1991. "Surface Roughness Effects on Soil Albedo." *Soil Science Society of America Journal* 64 (3): 1035–1041. doi:10.2136/sssaj2000.6431035x.

Mikhajlova, N. A., and D. S. Orlov. 1986. *Opticheskie Svoystva Pochv I Pochvennych Komponentov*, 118. Russia: Nauka.

Miller, P., W. Lanier, and S. Brandt. 2001. "Using Growing Degree Days to Predict Plant Stages." *Montana State University Extension Service* 9: MT00103 AG 7/2001.

Monfreda, C., N. Ramankutty, and J. A. Foley. 2008. "Farming the Planet: 2. Geographic Distribution of Crop Areas, Yields, Physiological Types, and Net Primary Production in the Year 2000." *Global Biogeochemical Cycles* 22 (1): 1–19. doi:10.1029/2007GB002947.

Monteith, J. L., and G. Szeicz. 1961. "The Radiation Balance of Bare Soil and Vegetation." *Quarterly Journal of the Royal Meteorological Society* 87 (372): 159–170. doi:10.1002/qj.49708737205.

NCAR (National Center for Atmospheric Research). 2017. "Research Data Archive." NCAR. Accessed October 17 2017. https://rda.ucar.edu

Oguntunde, P. G., A. E. Ajayi, and N. van de Giesen. 2006. "Tillage and Surface Moisture Effects on Bare-Soil Albedo of a Tropical Loamy Sand." *Soil and Tillage Research* 85 (1–2): 107–114. doi:10.1016/j.still.2004.12.009.

Oke, T. R. 1992. *Boundary Layer Climates*. 2nd ed. Taylor & Francis: New York.

Potter, K. N., R. Horton, and R. M. Cruse. 1987. "Soil Surface Roughness Effects on Radiation Reflectance and Soil Heat Flux1." *Soil Science Society of America Journal* 51 (4): 855. doi:10.2136/sssaj1987.03615995005100040003x.

Sacks, W. J., D. Deryng, J. A. Foley, and N. Ramankutty. 2010. "Crop Planting Dates: An Analysis of Global Patterns." *Global Ecology and Biogeography* 19 (5): 607–620. doi:10.1111/j.1466-8238.2010.00551.x.

Schneider, S. H., and R. E. Dickinson. 1974. "Climate Modeling." *Reviews of Geophysics* 12 (3): 447. doi:10.1029/RG012i003p00447.

Sellers, P. J., B. W. Meeson, F. G. Hall, G. Asrar, R. E. Murphy, R. A. Schiffer, F. P. Bretherton, et al. 1995. "Remote Sensing of the Land Surface for Studies of Global Change: Models — Algorithms — Experiments." *Remote Sensing of Environment* 51 (1): 3–26. doi:10.1016/0034-4257(94)00061-Q.

Taconet, O., and V. Ciarletti. 2007. "Estimating Soil Roughness Indices on a Ridge-and-Furrow Surface Using Stereo Photogrammetry." *Soil and Tillage Research* 93 (1): 64–76. doi:10.1016/j.still.2006.03.018.

Tóth, G., A. Jones, and L. Montanarella. 2013. "The LUCAS Topsoil Database and Derived Information on the Regional Variability of Cropland Topsoil Properties in the European Union." *Environmental Monitoring and Assessment* 185 (9): 7409–7425. doi:10.1007/s10661-013-3109-3.

USDA. 1994. "Major World Crop Areas and Climatic Profiles."." In *Agricultural Handbook. World Agricultural Outlook Board*. Washington: United States Department of Agriculture.

Vaudour, E., N. Baghdadi, and J. M. Gilliot. 2014. "Mapping Tillage Operations over a Peri-Urban Region Using Combined SPOT4 and ASAR/ENVISAT Images." *International Journal of Applied Earth Observation and Geoinformation* 28 (1): 43–59. doi:10.1016/j.jag.2013.11.005.

Viscarra Rossel, R. A., S. R. Cattle, A. Ortega, and Y. Fouad. 2009. "In Situ Measurements of Soil Colour, Mineral Composition and Clay Content by Vis-NIR Spectroscopy". *Geoderma* 150 (3–4). Elsevier B.V.: 253–266. doi:10.1016/j.geoderma.2009.01.025.

Viscarra Rossel, R. A., T. Behrens, E. Ben-Dor, D. J. Brown, J. A. M. Dematte, K. D. Shepherd, Z. Shi, et al. 2016. "A Global Spectral Library to Characterize the World's Soil." *Earth-Science Reviews* 155 (4): 198–230. doi:10.1016/j.earscirev.2016.01.012.

Wang, K., P. Wang, J. Liu, M. Sparrow, S. Haginoya, and X. Zhou. 2005. "Variation of Surface Albedo and Soil Thermal Parameters with Soil Moisture Content at a Semi-Desert Site on the Western Tibetan Plateau." *Boundary-Layer Meteorology* 116 (1): 117–129. doi:10.1007/s10546-004-7403-z.

Worthington, C., and C. Hutchinson. 2005. "Accumulated Growing Degree Days as a Model to Determine Key Developmental Stages and Evaluate Yield and Quality of Potato." *Proceedings of the Florida State Horticultural Society* 1: 98–101.